JOC The Journal of Organic Chemistry

pubs.acs.org/joc Article

Synthesis of a Series of Tropone-Fused Porphyrinoids

Emma K. Cramer and Timothy D. Lash*

Cite This: J. Org. Chem. 2022, 87, 952–962 Read Online

ACCESS | Metrics & More | Article Recommendations | Supporting Information

ABSTRACT: A series of tropone-fused porphyrinoids with unique spectroscopic features has been prepared. A dimethyl tropone-fused pyrrole was reacted with lead tetraacetate to give a bis(acetoxymethyl) derivative that condensed with an α-unsubstituted pyrrole *tert*-butyl ester to form a tripyrrane intermediate. Cleavage of the *tert*-butyl ester protective groups, followed by condensation with a series of aromatic dialdehydes and oxidation with DDQ, afforded the tropone-fused porphyrinoid systems. Reactions with pyrrole, furan, thiophene, and selenophene dialdehydes gave tropone-fused porphyrins and related heteroporphyrins. In addition, indene, 4-hydroxybenzene, and 3-hydroxypyridine dicarbaldehydes generated examples of carba-, oxybenzi-, and oxypyriporphyrins. The electronic absorption spectra of the tropone-fused porphyrinoids were greatly altered, showing shifts to longer wavelengths and the appearance of strong Q bands between 600 and 800 nm. The proton nuclear magnetic resonance spectra were also very unusual, as the internal protons were strongly shifted upfield, in some cases giving rise to resonances that approached −10 ppm. However, the external protons showed reduced downfield shifts compared to porphyrinoids that do not have tropone ring fusion. The profound changes observed for these macrocycles demonstrate that the introduction of fused tropone units, together with other structural changes such as core modification, can provide the means by which porphyrinoids with unique spectroscopic properties can be accessed.

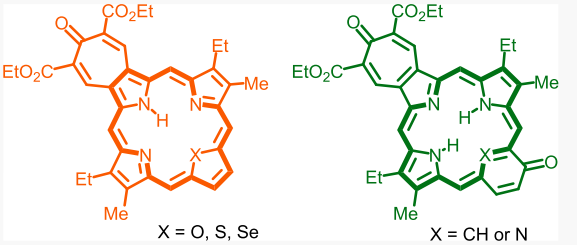

INTRODUCTION

Porphyrins have numerous biological functions[1] but are also being investigated for diverse applications that include sensor development,[2] optical materials,[3] catalysis,[4] dye-sensitized solar cells,[5] and photosensitizers for photodynamic therapy.[6] Modification of the electronic features of porphyrinoid systems has been accomplished using a variety of approaches including ring expansion[7] and contraction,[8] core modification,[9] ring fusion,[10] and *N*-alkylation.[11] Replacement of one or more of the core nitrogens with other heteroatoms such as O, S, Se,[9] and P[12] affords heteroporphyrins, while replacement with carbon atoms generates carbaporphyrins.[13] Carbaporphyrins such as **1** (Figure 1) retain fully aromatic porphyrin-like properties and have electronic absorption spectra that closely resemble those of regular porphyrins.[14] However, structurally related azuliporphyrins **2** have substantially reduced diatropic characteristics and produce very different electronic absorption spectra.[15] In particular, the UV−vis spectra of azuliporphyrins produce three medium-intensity bands between 350 and 450 nm together with a broad band at longer wavelengths, while benzocarbaporphyrin **1** gave a strong Soret band at 424 nm and a series of four Q bands. In an attempt to synthesize a methoxyazuliporphyrin **3** by the '3 + 1' condensation of a pyrrole dialdehyde **4** with azulitripyrrane **5**, spontaneous demethylation occurred generating a tropone-fused carbaporphyrin **6** (Scheme 1).[16] Unlike azuliporphyrins, the proton nuclear magnetic resonance (NMR) spectrum of **6** showed that the system possesses strongly diatropic properties. The

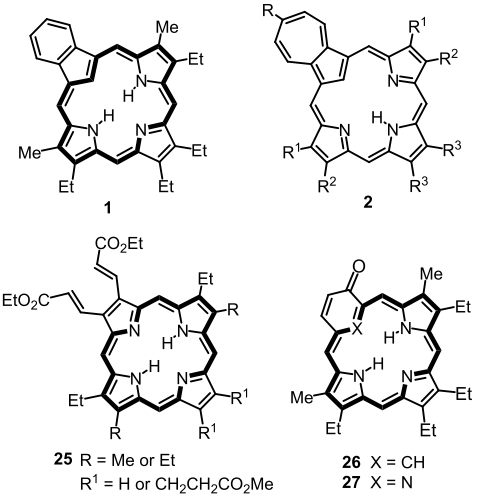

Figure 1. Structures of selected porphyrinoids.

Received: August 25, 2021
Published: January 12, 2022

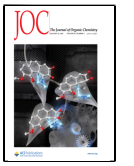

https://doi.org/10.1021/acs.joc.1c02063
J. Org. Chem. 2022, 87, 952−962

Scheme 1. Synthesis of a Tropone-Fused Carbaporphyrin

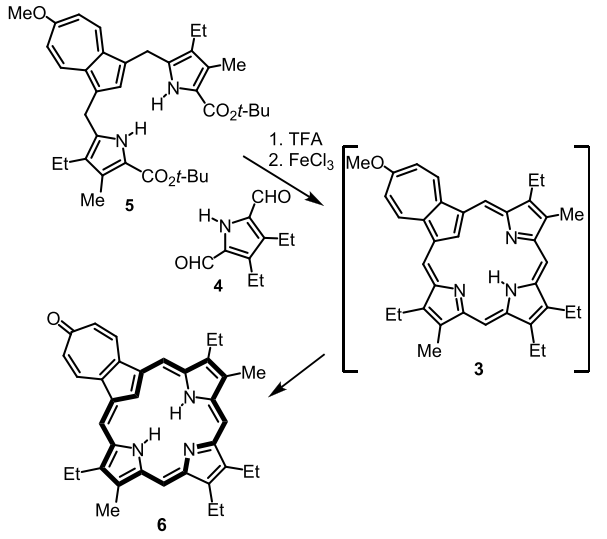

Scheme 2. Synthesis of a Tropone-Fused Tripyrrane

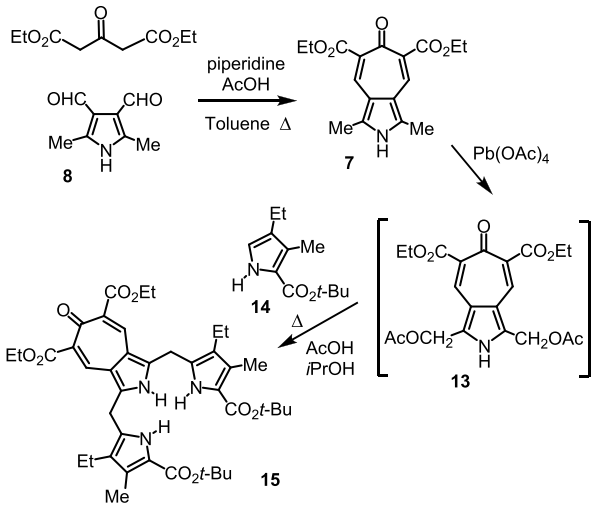

Scheme 3. Synthesis of Tripyrranes with Electron-Withdrawing Acrylate Units

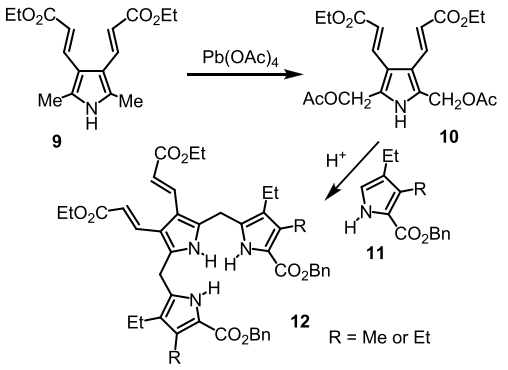

meso-protons gave rise to two 2H downfield singlets at 9.26 and 9.40 ppm, while the internal CH and NH resonances appeared upfield at −7.64 and −4.47 ppm, respectively.[16] Nevertheless, the UV−vis spectrum of **6** was highly modified showing multiple medium-intensity bands in the Soret region that resembled the spectra of azuliporphyrins, but with a series of Q type bands that were similar to those seen for porphyrins and carbaporphyrins such as **1**.

Given the unique hybrid properties of tropone-fused carbaporphyrin **6**, the synthesis of other examples of tropone-fused porphyrinoids was considered to be a worthwhile goal. In this paper, the synthesis of a series of porphyrinoids with tropone rings fused to pyrrolic subunits is reported. These novel structures exhibit considerably modified electronic absorption spectra while retaining macrocyclic aromaticity.

RESULTS AND DISCUSSION

To access a series of tropone-fused macrocycles, a suitable pyrrolic building block was required. Two groups independently investigated the synthesis of cyclohepta[*c*]pyrrole-6-ones such as **7** (Scheme 2).[17,18] We adapted these studies and reacted pyrrole dialdehyde **8** with diethyl 1,3-acetonedicarboxylate in toluene with catalytic piperidine and acetic acid under Dean−Stark conditions[19] and isolated tropone-fused pyrrole **7** in 84% yield. To synthesize porphyrin-type systems, it was necessary to derivatize the two α-methyl substituents. Boudif and Momenteau demonstrated that 2,5-dimethylpyrrole **9** with two electron-withdrawing acrylate substituents reacted with lead tetraacetate in acetic acid to give bis(acetoxymethyl)-pyrrole **10**, and this condensed with α-unsubstituted pyrroles **11** under acidic conditions to afford tripyrranes **12** (Scheme 3).[20] Tropone-fused pyrrole **7** also reacted with lead tetraacetate to give diacetate **13**, but this derivative could not be isolated in pure form. Instead, crude **13** was condensed with α-unsubstituted pyrrole *tert*-butyl ester **14** in refluxing isopropyl alcohol containing acetic acid to give tripyrrane **15**. The tripyrrane could not be purified by column chromatography as extensive decomposition occurred. However, recrystallization from isopropyl alcohol gave reasonably pure **15** in 34% (two steps) from **7**.

Tripyrrane **15** was condensed with a series of aromatic dialdehydes in the presence of TFA to generate macrocyclic products (Scheme 4) using the '3 + 1' methodology.[21] Reaction of **15** with pyrrole dialdehyde **4**, followed by oxidation with DDQ, gave tropone-fused porphyrin **16** in 57−71% yield. We recently reported improved syntheses of heteroporphyrins and *N*-alkylated derivatives by application of the '3 + 1' strategy[11] and have applied this approach to the synthesis of tropone-fused heteroporphyrins. Hence, furan, thiophene, or selenophene dialdehydes **17a−c** were reacted with tripyrrrane **15** to afford heteroporphyrins **18−20**, respectively, in 50−76% yield. In addition, the methodology was well suited for the synthesis of porphyrin analogues **21−23** (Scheme 4). Reaction of **15** with indene dialdehyde **24** under the same conditions afforded benzocarbaporphyrin **21** in 49% yield. Tripyrrane **15** reacted similarly with 4-hydroxyisophthaladehyde (**25a**) to generate oxybenziporphyrin **22** in 65% yield, while the analogous pyridine dialdehyde **25b** produced oxypyriporphyrin **23** in 57% yield. All of the products were purified by column chromatography followed by recrystallization. Attempts to purify porphyrin **16** on grade 3 alumina led to extensive losses, but superior results were obtained on silica gel, and the product was eluted as a dark green fraction with 1% methanol-chloroform. Porphyrin analogues **18−23** were all purified on grade 3 basic alumina, although the polarity of these products varied considerably. Thia- and selenaporphyrins traveled through the columns with dichloromethane or a 1:1

https://doi.org/10.1021/acs.joc.1c02063
J. Org. Chem. 2022, 87, 952−962

Scheme 4. Synthesis of a Series of Tropone-Fused Porphyrinoids

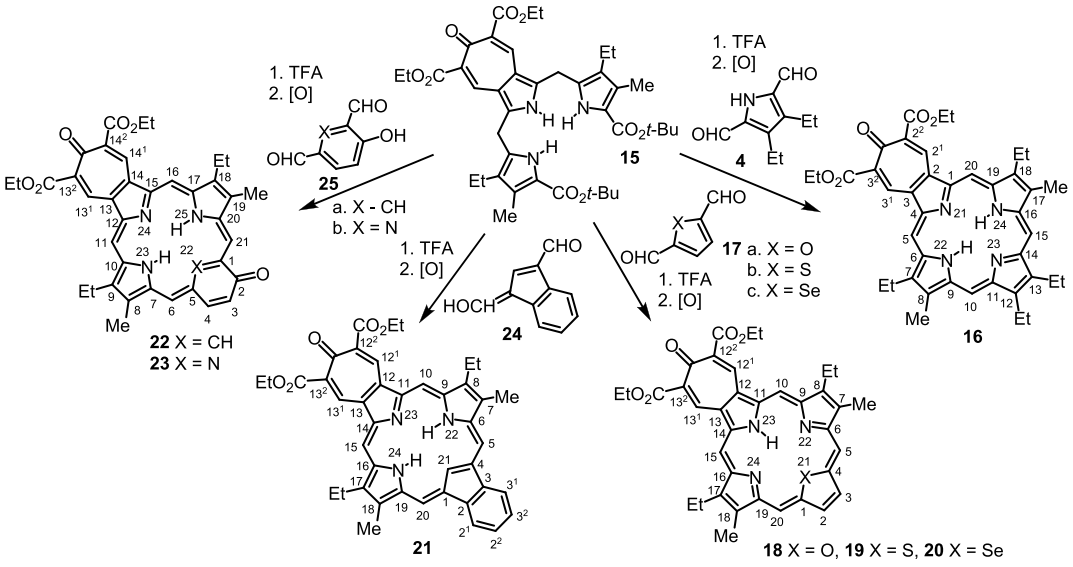

mixture of dichloromethane and chloroform, but oxaporphyrin was far more polar and required 1% methanol-chloroform to elute. Oxybenziporphyrin **22** and oxypyriporphyrin **23** exhibited intermediary polarity and were eluted with chloroform.

The ^{1}H NMR spectrum of porphyrin **16** in $CDCl_3$ was consistent with that of an aromatic compound, although there were some atypical features (Figure 2). The internal NH

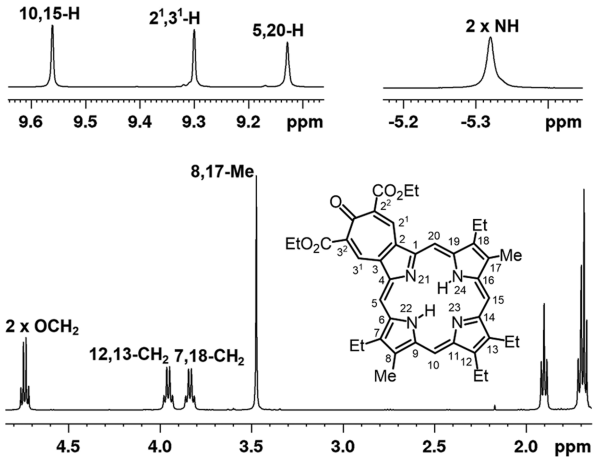

Figure 2. ^{1}H NMR spectrum of tropone-fused porphyrin **16** in $CDCl_3$.

protons of porphyrins are typically observed between −3 and −4 ppm,[22] but this resonance shifted further upfield for **16**. The precise value varied with concentration but was observed between −4.7 and −5.4 ppm. On the other hand, the *meso*-protons were not shifted as far downfield as regular porphyrins, giving rise to two 2H singlets at 9.70 and 9.54 ppm (again some variations in these values were noted). The UV−vis spectrum of **16** was also unusual (Figure 3). *meso*-Unsubstituted porphyrins generally give a Soret band near 400 nm and a series of four much smaller Q bands between 490 and 625 nm. In contrast, tropone-fused porphyrin **16** gave two Soret bands at 376 and 439 nm and two relatively strong Q bands at 588 and 615 nm. These spectroscopic properties

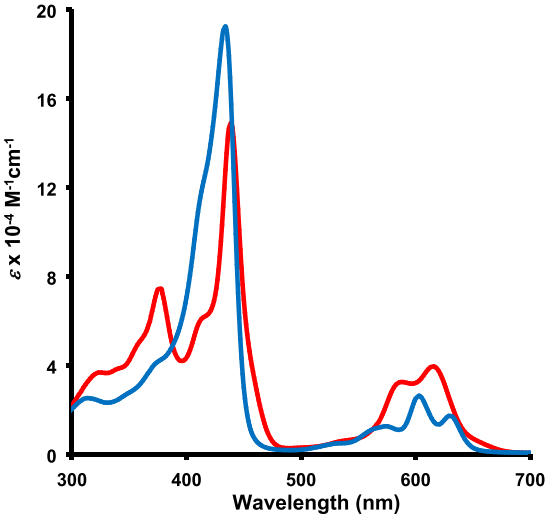

Figure 3. UV−vis spectra of tropone-fused porphyrin **16** (7.034×10^{-6} M) in CH_2Cl_2 (red line) and with 400 equiv TFA in CH_2Cl_2 (blue line).

do not simply arise from the presence of an electron-withdrawing unit as porphyrins **25** (Figure 1) with two strongly electron-withdrawing acrylate substituents do not show particularly unusual properties.[20] In particular, these showed a single strong Soret band near 428 nm and a series of four Q bands.[20] The *meso*-protons for porphyrins **25** appeared near 10 ppm, while the NH resonances showed up between −3.6 and −4.2 ppm, values that are typical of *meso*-unsubstituted porphyrins but significantly different from **16**. Protonation of **16** was also investigated (Scheme 5). Spectrophotometric titration with TFA revealed that the electron-withdrawing tropone unit greatly reduces the basicity of the porphyrin and complete monoprotonation required the addition of 400 equivalents of TFA. The resulting species gave an intense Soret band at 438 nm ($\varepsilon = 1.92 \times 10^5$) and three Q bands at 574, 603, and 630 nm (Figure 3). Further changes were noted at higher acid concentrations, and in 20% TFA (3.83×10^5 equiv TFA), a new band emerged at 684 nm. Although Scheme 5 indicates that protonation occurs on the

https://doi.org/10.1021/acs.joc.1c02063
J. Org. Chem. 2022, 87, 952−962

Scheme 5. Protonation of Tropone-Fused Porphyrinoids

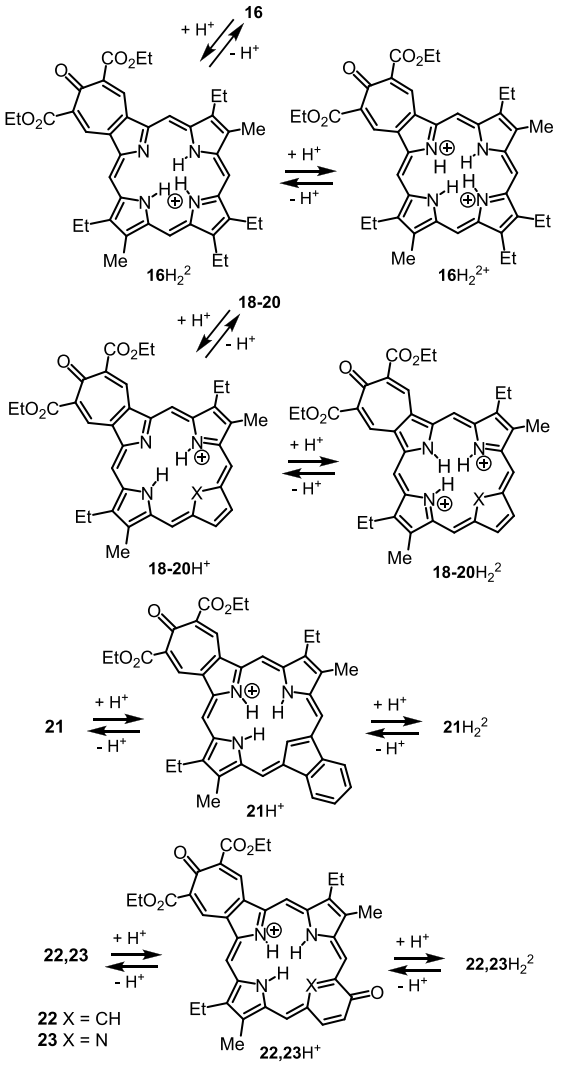

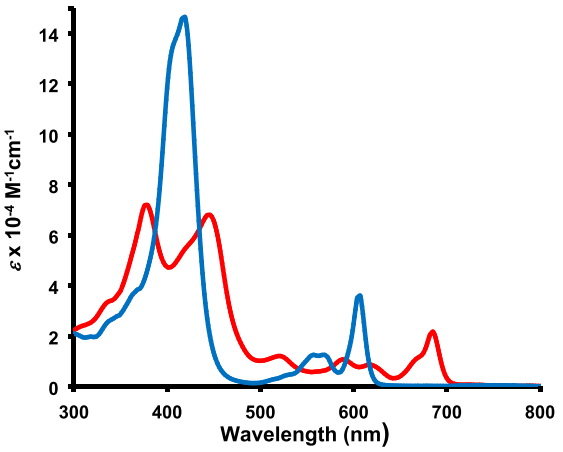

Figure 4. UV−vis spectra of tropone-fused oxaporphyrin **18** (1.479×10^{-5} M) in 1% Et_3N-CH_2Cl_2 (red line) and in CH_2Cl_2 with 2 equiv TFA (blue line).

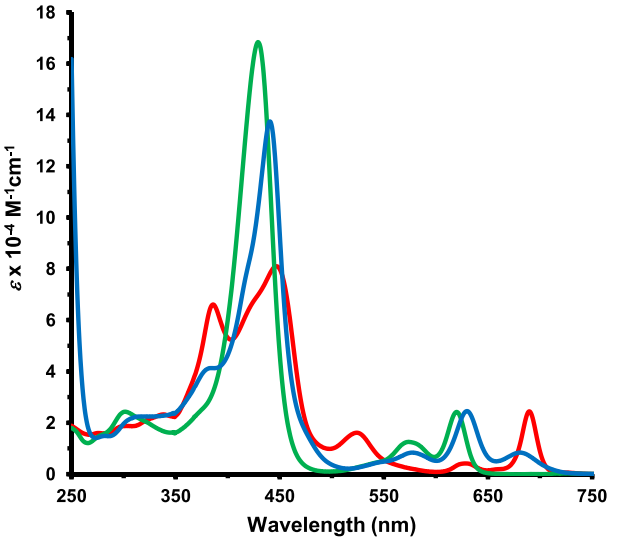

Figure 5. UV−vis spectrum of tropone-fused thiaporphyrin **19** (1.554×10^{-5} M) in CH_2Cl_2 (red line), in CH_2Cl_2 with 100 equiv TFA (green line), and in 20% TFA-CH_2Cl_2 (1.73×10^5 equiv TFA, blue line).

pyrrolenine nitrogens, protonation could take place on the tropone-carbonyl unit instead as this would give the seven-membered ring a favorable hydroxytropylium ion character.[23] Further studies will be required to confirm the identity of the protonated species.

Oxaporphyrin **18** protonated very easily, and solutions of **18** in CH_2Cl_2 were partially or fully monoprotonated even when the solvent was deacidified with basic alumina (Scheme 5). The free base in 1% Et_3N-CH_2Cl_2 gave two broad Soret bands at 378 and 445 nm and a series of Q bands, including a medium-intensity absorption at 685 nm (Figure 4). However, dilute solutions of free base **15** were somewhat unstable and slowly decomposed when exposed to light. In CH_2Cl_2 with 1 or 2 equiv of TFA, **18**H$^+$ gave a strong Soret band at 418 nm and Q bands at 556, 568, and 606 nm (Figure 4). Further protonation only occurred at much higher concentrations of TFA, and in 20% TFA (1.82×10^5 equiv TFA), the Soret band shifted to 433 nm while a long-wavelength absorption emerged at 672 nm (Figures S13 and S14). Thia- and selenaporphyrins **19** and **20** were more resistant to monoprotonation. The free base form of **19** in CH_2Cl_2 gave two Soret bands at 386 and 447 nm and a moderately strong Q band at 690 nm (Figure 5), whereas **20** afforded Soret bands at 387 and 446 nm and a long-wavelength Q band at 689 nm (Figure 6). These spectra are substantially altered, and the bands strongly red shifted compared to structures without fused tropone rings. In the absence of the tropone unit, there are no strong long-wavelength absorptions and only one Soret band is present near 400 nm.[11] Addition of TFA to solutions of **19** or **20** in CH_2Cl_2 gave rise to monocationic species, but it was necessary to add 50 equiv of TFA to complete the transformation to **19**H$^+$ and >400 equiv to form **20**H$^+$. Monocation **19**H$^+$ gave a strong Soret band at 429 nm and Q bands at 574 and 620 nm (Figure 5), while **20**H$^+$ produced a Soret band at 453 nm and longer wavelength absorptions at 593 and 645 nm (Figure 6). At higher concentrations of TFA, further spectroscopic changes were noted. Thiaporphyrin **19** in 20% TFA-CH_2Cl_2 (1.73×10^5 equiv TFA) gave a new absorption at 681 nm and the Soret band shifted to 441 nm, while selenaporphyrin **20** in 40% TFA-CH_2Cl_2 (3.31×10^5 equiv TFA) gave a Soret band at 458 nm and a long-wavelength band at 694 nm. These changes were attributed to the formation of diprotonated species **19,20**H_2^{2+}.

https://doi.org/10.1021/acs.joc.1c02063
J. Org. Chem. 2022, 87, 952−962

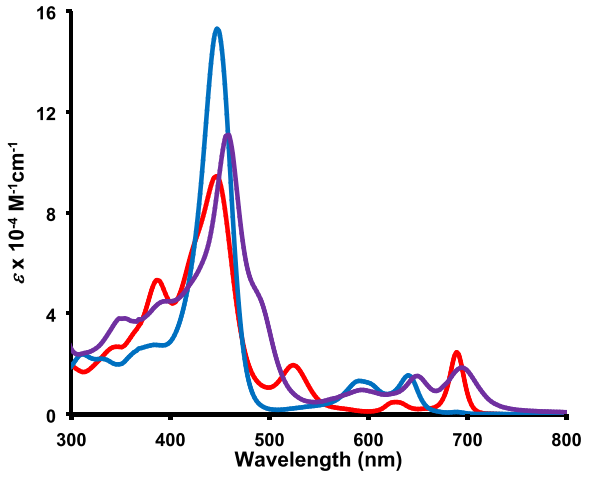

Figure 6. UV−vis spectra of tropone-fused selenaporphyrin **20** (1.628×10^{-5} M) in CH_2Cl_2 (red line), in CH_2Cl_2 with 400 equiv TFA (blue line), and in 40% TFA-CH_2Cl_2 (3.31×10^5 equiv TFA, purple line).

The ^{1}H NMR spectra of core modified porphyrins **18**−**20** were also insightful. The poor solubility of oxaporphyrin **18** in $CDCl_3$ made it difficult to obtain high-quality spectra, but in TFA-$CDCl_3$ the internal NH protons gave rise to an atypically upfield resonance at −5.5 ppm, while the *meso*-protons were shifted downfield to give two 2H peaks at 11.12 and 11.08 ppm. Superior results were obtained for spectra run in TFA-DMSO-d_6. In this solvent mixture, the NH signals appeared at a remarkably upfield value of −8.93 ppm and the *meso*-protons were again strongly deshielded to give resonances at 10.29 and 10.12 ppm. The furan protons were identified at 10.29 ppm, clearly demonstrating that the macrocyclic ring current passes through the periphery of the furan subunit. The tropone-protons were also strongly deshielded, appearing at 9.88 ppm, because of their proximity to the macrocyclic π-system and the ester carbonyl units. Thiaporphyrin **19** in $CDCl_3$ gave a broad upfield peak between −4.1 and −4.6 ppm for the NH and the *meso*-protons appeared at 10.38 and 9.38 ppm. In addition, the thiophene protons were located at 9.98 ppm. These data are consistent with a strong aromatic system. In TFA-$CDCl_3$, the protonated form gave resonances for the *meso*-protons at 11.53 and 11.23 ppm, while the thiophene protons were present at 10.61 ppm, indicating that the diatropicity has been enhanced. The ^{1}H NMR spectrum of selenaporphyrin **20** in $CDCl_3$ indicated that the diatropic ring current was slightly reduced as the *meso*-protons were shifted upfield compared to **19** to give peaks at 10.19 and 8.50 ppm, while the thiophene protons appeared at 10.04 ppm. Nevertheless, the NH resonance was still strongly shifted upfield to −5.45 ppm. Protonation increased the diamagnetic ring current, and the *meso*-protons shifted downfield to 11.53 and 11.13 ppm, while the selenophene protons appeared at 10.40 ppm. The symmetry of these macrocycles was evident from both the ^{1}H and ^{13}C NMR spectra (although the placement of the NH proton in **19** and **20** technically breaks the symmetry, rapid tautomerization results in the apparent symmetry observed). In the ^{13}C NMR spectra, the *meso*-protons for free base thiaporphyrin **19** were identified at 113.2 and 98.1 ppm, while selenaporphyrin **20** gave these peaks at 116.3 and 98.3 ppm.

The ^{1}H NMR spectrum of benzocarbaporphyrin **21** in $CDCl_3$ showed the *meso*-protons at 9.04 and 8.50 ppm, and these values indicate that the macrocyclic ring current has been reduced because of the presence of the fused tropone unit as benzocarbaporphyrin **1** gives the equivalent resonances further downfield at 9.82 and 10.10 ppm.[14] However, the internal NHs afforded a broad resonance near −7 ppm, while the internal CH could be identified between −9.29 and −9.64 ppm (Figure 7). These upfield shifts are unusual as the NH and CH

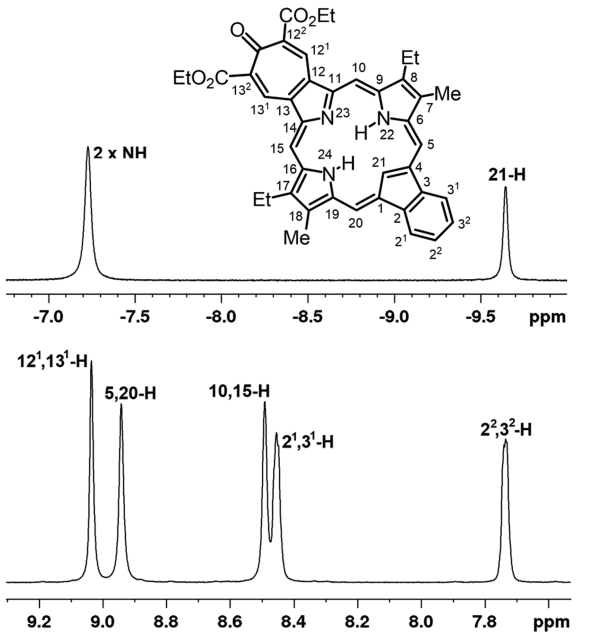

Figure 7. Partial ^{1}H NMR spectrum of tropone-fused benzocarbaporphyrin **21** in $CDCl_3$ at 55 °C showing the upfield and downfield regions. The spectrum was run at an elevated temperature because of the poor solubility of **21**.

resonances in benzocarbaporphyrins such as **1** are observed at ca. −4 ppm and −6.8 ppm, respectively.[14] The benzo-protons for **21** were observed as two 2H multiplets at 8.5 and 7.8 ppm, and this result indicates that the fused benzene ring is not involved in global delocalization pathways. The ^{13}C NMR spectrum again confirmed the symmetry of this structure and gave two peaks for the *meso*-carbons at 97.6 and 93.5 ppm. The internal carbon resonance was identified at 108.6 ppm. The ^{1}H NMR spectrum of **21** in TFA-$CDCl_3$ showed that the resulting protonated species had a much stronger macrocyclic ring current as the *meso*-protons shifted downfield to afford two 2H singlets at 10.42 and 10.20 ppm, while the internal CH appeared upfield at −6.31 ppm. The UV−vis spectrum of **21** in CH_2Cl_2 was highly modified compared to that of benzocarbaporphyrins such as **1**. The UV−vis spectrum of **1** gives a strong Soret band at 424 nm, together with a series of weak Q bands at 510, 544, 602, and 662 nm (the longest wavelength Q band has a particularly low intensity).[14] However, **21** gave a Soret band at 460 nm and abnormally strong red shifted Q bands at 610 and 652 nm (Figure 8). A weaker absorption also appeared at 711 nm. Addition of TFA led to spectroscopic changes, and with 500 equivalents of TFA, the UV−vis spectrum showed a weakened Soret band at 473 nm and broad absorptions at longer wavelengths (Figure 8). Unfortunately, dilute solutions of protonated **21** rapidly decomposed when exposed to ambient laboratory lighting, and this factor limited this type of investigation.

https://doi.org/10.1021/acs.joc.1c02063
J. Org. Chem. 2022, 87, 952−962

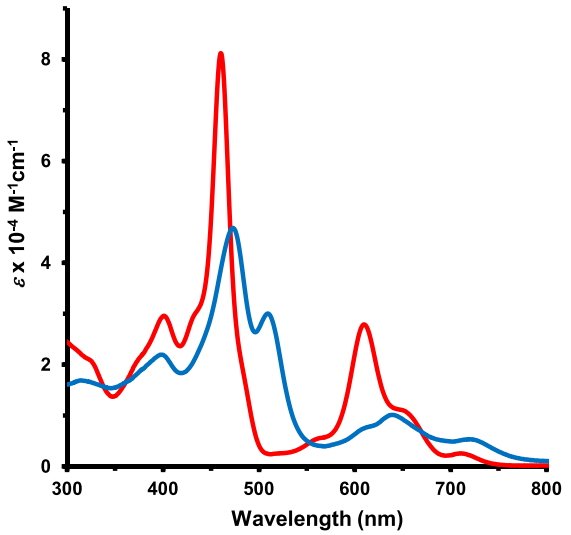

Figure 8. UV−vis spectra of tropone-fused benzocarbaporphyrin **21** (1.001×10^{-5} M) in CH_2Cl_2 (red line) and with 500 equiv TFA in CH_2Cl_2 (blue line).

Oxybenziporphyrin **22** also has unusual spectroscopic properties. The ^{1}H NMR spectrum of **22** in $CDCl_3$ showed that the NH protons strongly shifted upfield to −6.24 and −6.59 ppm, while the internal CH appeared between −9.1 and −9.5 ppm (Figure 9). This contrasts with oxybenziporphyrin

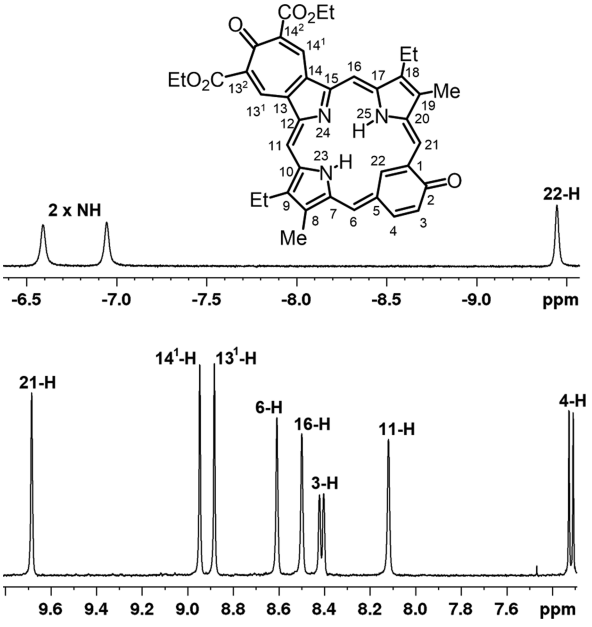

Figure 9. Partial ^{1}H NMR spectrum of tropone-fused oxybenziporphyrin **22** in $CDCl_3$ showing the upfield and downfield regions.

26 (Figure 1) which shows the NH protons as a broad resonance close to −4 ppm and the inner CH at −7.2 ppm.[24] However, the *meso*-protons in **22** gave rise to four 1H singlets at 9.81, 8.74, 8.67, and 8.29 ppm, values that are approximately 0.4 ppm upfield from those reported for oxybenziporphyrin **26**. The ^{13}C NMR spectrum of **22** showed the *meso*-carbon resonances at 111.0, 105.0, 94.2, and 91.8 ppm, while the inner CH appeared at 111.8 ppm. In TFA-$CDCl_3$, the *meso*-carbon resonances shifted significantly downfield with the 21-H appearing at 9.94 ppm. This again differs from **26** which shows greatly reduced diatropicity under these conditions because of the formation of a phenolic dication. Nevertheless, the inner CH resonance for **22** shifted downfield to −1.08 ppm. The UV−vis spectrum of **22** was also very different from that of **26**. In regular oxybenziporphyrin, the Soret band at 428 nm is accompanied by a smaller peak at 456 nm.[24] This is followed by a series of Q bands at 548, 590, 636, and 698 nm. In **22**, the Soret band appearing at 448 nm is accompanied by distinct shoulders on either side (Figure 10). Importantly,

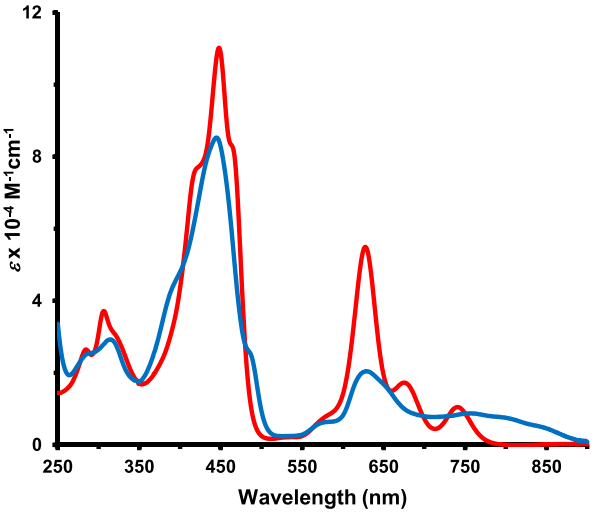

Figure 10. UV−vis spectra of tropone-fused oxybenziporphyrin **22** (1.948×10^{-5} M) in CH_2Cl_2 (red line) and 1% TFA-CH_2Cl_2 (6.91×10^3 equiv, blue line).

three relatively strong bathochromically shifted Q bands are seen at 627, 676, and 741 nm. Addition of TFA led to gradual changes in the UV−vis spectra. In 10% TFA-chloroform (6.91×10^4 equiv TFA), a Soret band was seen at 443 nm, together with Q bands at 582, 634, 728, and 804 nm. This was attributed to the formation of **22**H$^+$ (Scheme 5).

Oxypyriporphyrin **23** shows many of the same trends. The ^{1}H NMR spectrum of **23** in $CDCl_3$ gave two broad upfield peaks for the NH protons at −6.04 and −6.28 ppm, while the *meso*-protons gave rise to four 1H singlets at 10.26, 9.25, 8.95, and 8.80 ppm (Figure 11). The *meso*-protons in oxypyriporphyrin **27** (Figure 1) are much further downfield, appearing at 10.90, 9.72, 9.70, and 9.48 ppm, but the internal NHs give rise to a broad peak at −3.59 ppm.[24] The ^{13}C NMR spectrum showed the keto-units at 185.0 and 184.4 ppm, while the *meso*-carbons gave rise to four separate signals at 107.7, 102.5, 95.7, and 95.0 ppm. When the ^{1}H NMR spectrum of **23** was run in TFA-$CDCl_3$, the protonated species showed enhanced diatropicity and the *meso*-protons shifted downfield to give four resonances at 10.79, 10.32, 10.29, and 9.82 ppm. The UV-spectrum of pyriporphyrins such as **27** gave Soret bands at 422 nm and a series of Q bands at 548, 586, 609, and 661 nm, although the longest wavelength absorption is very weak.[24] In contrast, **23** gave Soret bands at 414 and 442 nm and two strong Q bands at 616 and 651 nm (Figure 12). Addition of TFA to solutions of **23** initially showed only minor changes, but in the presence of 1000 equiv of TFA, the Soret band was less intense and Q bands were seen at 623, 658, and 739 nm (Figure 12). This species was assigned to monocation **23**H$^+$. At higher concentrations of TFA, further changes were

https://doi.org/10.1021/acs.joc.1c02063
J. Org. Chem. 2022, 87, 952−962

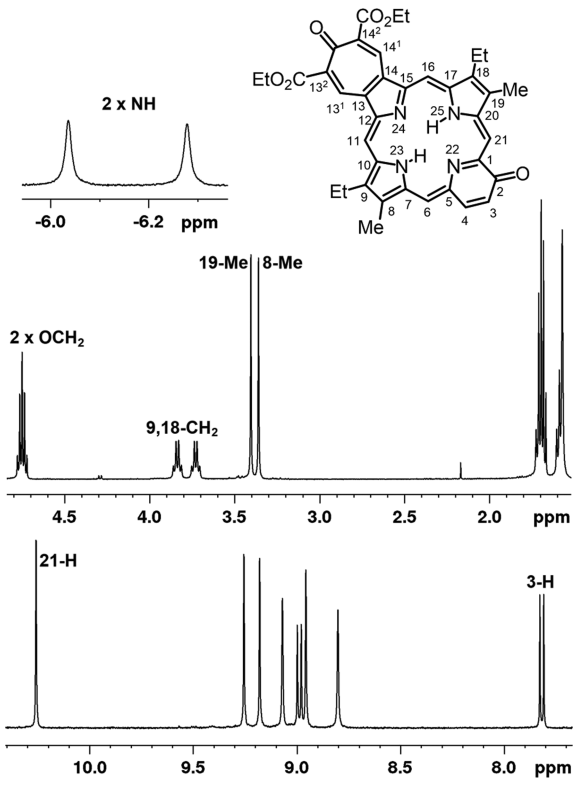

Figure 11. ^{1}H NMR spectrum of tropone-fused oxypyriporphyrin **23** in $CDCl_3$.

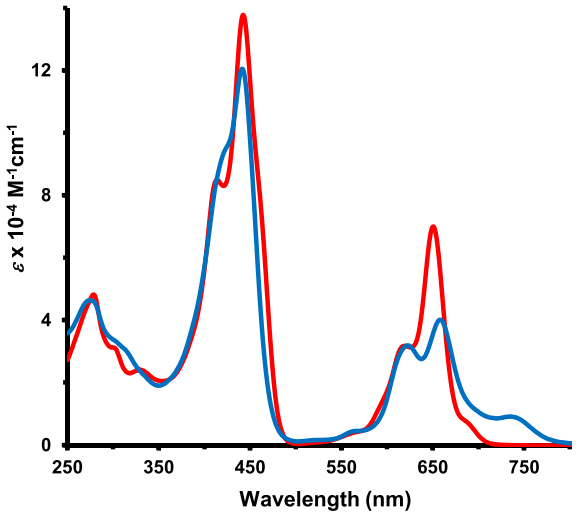

Figure 12. UV−vis spectra of tropone-fused oxypyriporphyrin **23** (8.554×10^{-6} M) in CH_2Cl_2 (red line) and with 1000 equiv TFA in CH_2Cl_2 (blue line).

observed, and in 40% TFA-CH_2Cl_2 (6.29×10^5 equiv TFA), the Soret band shifted to 448 nm and Q bands appeared at 581, 618, 683, and 761 nm. Once more, the porphyrinoid macrocycle has greatly reduced basicity because of the presence of the fused tropone unit.

CONCLUSIONS

Fusion of tropone units onto a series of porphyrinoid structures led to profound changes to their proton NMR and electronic absorption spectra. The UV−vis spectra showed significant bathochromic shifts and the presence of unusually strong Q bands. In the proton NMR spectra, the internal protons appeared in a remarkably upfield region, in some cases giving resonances that approached −10 ppm. However, the external protons exhibited reduced downfield shifts consistent with a reduction in macrocyclic diatropicity. The electron-withdrawing tropone unit also led to decreased basicity for these structures, and monoprotonated species were easily identified. These results demonstrate that a combination of core modification and ring fusion, together with other structural modifications, can lead to porphyrinoid systems with remarkably altered properties.

EXPERIMENTAL SECTION

Melting points are uncorrected. NMR spectra were recorded using a 400 or 500 MHz NMR spectrometer and were run at 302 K unless otherwise indicated. ^{1}H NMR values are reported as chemical shifts δ, relative integral, multiplicity (s, singlet; d, doublet; t, triplet; q, quartet; m, multiplet; br, broad peak), and coupling constant (J). Chemical shifts are reported in parts per million (ppm) relative to $CDCl_3$ (^{1}H residual $CHCl_3$ singlet δ 7.26 ppm, ^{13}C $CDCl_3$ triplet δ 77.23 ppm) or DMSO-d_6 (^{1}H residual DMSO-d_5 pentet δ 2.49 ppm, ^{13}C DMSO-d_6 septet δ 39.7 ppm), and coupling constants were taken directly from the spectra. NMR assignments were made with the aid of ^{1}H-^{1}H COSY, HSQC, DEPT-135, and nOe difference proton NMR spectroscopy. 2D-NMR experiments were performed using standard software. Mass spectral data were acquired using positive-mode electrospray ionization (ESI^+) and a high-resolution time-of-flight mass spectrometer.

Diethyl 1,3-dimethyl-2*H*-cyclohepta[*c*]pyrrole-6-one-3,7-dicarboxylate (7). Piperidine (0.5 mL) and acetic acid (1.3 mL) were added to a solution of 2,5-dimethyl-3,4-pyrroledicarbaldehyde[20,25] (1.032 g, 6.83 mmol) and diethyl-1,3-acetonedicarboxylate (1.554 g, 9.1 mmol) in toluene (60 mL). A Dean−Stark apparatus was attached to the flask, and the mixture was heated using an oil bath under reflux with azeotropic removal of water overnight. The resulting precipitate was suction-filtered to give the tropone-fused pyrrole (1.830 g, 5.77 mmol, 84%) as an off-white solid, mp 245.5−247 °C, dec (lit. mp[17] 255−258 °C). ^{1}H NMR (500 MHz, DMSO-d_6): δ 12.36 (br s, 1H, NH), 7.75 (s, 2H, 2 × tropone-H), 4.19 (q, 4H, J = 7.1 Hz, 2 × OCH_2), 2.42 (s, 6H, 2 × pyrrole-CH_3), 1.25 (t, 6H, J = 7.1 Hz, 2 × OCH_2CH_3). ^{13}C{^{1}H} NMR (125 MHz, DMSO-d_6): δ 184.3, 168.4, 133.7 (2 × tropone-CH), 133.6, 129.2, 116.6, 60.9 (2 × OCH_2), 14.5 (2 × OCH_2CH_3), 10.9 (2 × pyrrole-CH_3).

Tropone-Fused Tripyrrane 15. A suspension of tropone-fused pyrrole 7 (0.548 g, 1.73 mmol) in acetic acid (25 mL) was stirred with lead tetraacetate (95%, 1.643 g, 3.52 mmol) at room temperature overnight. The solid was slowly dissolved to give a yellow solution. The solution was poured into ice-water (200 mL), extracted with ethyl acetate (4 × 50 mL), and washed with 5% sodium bicarbonate solution. The solution was dried over magnesium sulfate and evaporated under reduced pressure. The solid residue was dissolved in isopropyl alcohol (15 mL) with *tert*-butyl 4-ethyl-3-methylpyrrole-2-carboxylate[26] (650 mg, 3.11 mmol) and acetic acid (1 mL), and the mixture was refluxed under nitrogen overnight. The solvents were removed on a rotary evaporator, and the residue was taken up in hot isopropyl alcohol (9 mL). The mixture was allowed to cool to room temperature and then placed in a freezer for 1 h. The resulting precipitate was suction-filtered and washed with cold isopropyl alcohol (7−8 mL) to give the tripyrrane (425 mg, 0.581 mmol, 34% from 7) as an off-white or pale yellow solid, mp 210−212 °C, dec. ^{1}H NMR (500 MHz, $CDCl_3$): δ 10.02 (1H, br s, NH), 9.64 (2H, br s, 2 × NH), 8.00 (2H, 2 × tropone-H), 4.31 (4H, q, J = 7.4 Hz, 2 × OCH_2CH_3), 4.10 (4H, s, 2 × bridge-CH_2), 2.31 (4H, q, J = 7.4 Hz, pyrrole-CH_2CH_3), 2.18 (6H, s, 2 × pyrrole-CH_3), 1.51 (18H, s, 2 × O*t*-Bu), 1.33 (6H, t, J = 7.2 Hz, 2 × OCH_2CH_3), 0.87 (6H, t, J = 7.4 Hz, 2 × pyrrole-CH_2CH_3). ^{13}C{^{1}H} NMR (125 MHz, $CDCl_3$, 328 K): δ 185.7, 168.0, 161.3, 133.3 (2 × tropone-CH), 132.9, 130.4, 126.3, 126.0, 125.2, 120.5, 117.5, 80.8 (2 × $OCMe_3$), 61.6 (2 ×

https://doi.org/10.1021/acs.joc.1c02063
J. Org. Chem. 2022, 87, 952−962

OCH_3), 28.8 (2 × *t*-Bu), 22.9 (2 × bridge-CH_2), 17.4 (2 × pyrrole-CH_2CH_3), 15.4 (2 × pyrrole-CH_2CH_3), 14.4 (2 × OCH_2CH_3), 10.6 (2 × pyrrole-CH_3). ^{1}H NMR (500 MHz, DMSO-d_6): δ 12.00 (s, 1H, NH), 10.92 (s, 2H, 2 × NH), 7.80 (s, 2H), 2 × tropone-H), 4.18−4.14 (overlapping s and q, 8H, 2 × OCH_2 and 2 × bridge-CH_2), 2.22 (q, 4H, J = 7.5 Hz, 2 × pyrrole-CH_2CH_3), 2.11 (s, 6H, 2 × pyrrole-CH_3), 1.49 (s, 18H, 2 × *t*-Bu), 1.23 (t, 6H, J = 7.1 Hz, 2 × OCH_2CH_3), 0.71 (t, 6H, J = 7.5 Hz, 2 × pyrrole-CH_2CH_3). ^{13}C{^{1}H} NMR (125 MHz, DMSO-d_6): δ 183.9, 167.5, 160.8, 134.5, 133.0 (2 × tropone-CH, 129.7, 128.5, 124.8, 123.2, 118.4, 116.1, 79.3 (2 × $OCMe_3$), 60.6 (2 × OCH_3), 28.3 (2 × *t*-Bu), 22.0 (2 × bridge-CH_2), 16.7 (2 × pyrrole-CH_2CH_3), 15.2 (2 × pyrrole-CH_2CH_3), 14.1 (2 × OCH_2CH_3), 10.4 (2 × pyrrole-CH_3). HRMS (ESI) m/z: $[M + H]^+$ calcd for $C_{41}H_{54}N_3O_9$ 732.3860, found 732.3837.

Tropone-Fused Porphyrin 16. Tropone-fused tripyrrane **15** (53.0 mg, 0.0725 mmol) was stirred with TFA (1 mL) in a pear-shaped flask under nitrogen for 10 min. Dichloromethane (40 mL) was added followed by 3,4-diethyl-2,5-pyrroledicarbaldehyde[27] (13.0 mg, 0.0726 mmol), and the mixture was stirred under nitrogen in the dark overnight. The solution was neutralized with triethylamine,[28] DDQ (98%, 17 mg, 0.073 mmol) was added, and the resulting mixture was stirred for 30 min. The solution was washed with water, and the organic layer was evaporated under reduced pressure. The residue was purified by column chromatography on silica, eluting with chloroform and then 1% methanol-chloroform, to give a dark green band. Recrystallization with chloroform-hexanes gave the tropone-fused porphyrin (27.6 mg, 0.0411 mmol, 57%) as a dark green solid, mp > 300 °C. UV−vis (CH_2Cl_2; 7.034 × 10^{-6} M): λ_{max}/nm (log ε): 323 (sh, 4.56), 376 (4.87), 413 (sh, 4.79), 439 (5.17), 536 (sh, 3.77), 588 (4.51), 615 (4.60). UV−vis (400 equiv TFA-CH_2Cl_2): λ_{max}/nm (log ε): 314 (4.40), 373 (sh, 4.61), 434 (5.28), 574 (4.10), 603 (4.42), 630 (4.24). UV−vis (1% TFA-CH_2Cl_2; 1.91 × 10^4 equiv): λ_{max}/nm (log ε): 312 (sh, 4.28), 413 (sh, 5.00), 435 (5.37), 535 (sh, 3.59), 560 (sh, 3.96), 577 (4.02), 632 (4.45). ^{1}H NMR (500 MHz, $CDCl_3$): δ 9.56 (s, 2H, 10,15-H), 9.30 (s, 2H, 3^1,2^1-H), 9.13 (s,2H, 5,20-H), 4.74 (q, 4H, J = 7.2 Hz, 2 × OCH_2), 3.96 (q, 4H, J = 7.7 Hz, 12,13-CH_2), 3.84 (q, 4H, J = 7.7 Hz, 7,18-CH_2), 3.47 (s, 6H, 8,17-CH_3), 1.90 (t, 6H, J = 7.7 Hz), 1.71−1.67 (2 overlapping triplets, 12H) (7,12,13,18-CH_2CH_3 and 2 × OCH_2CH_3), −5.32 (br s, 2H, 2 × NH). ^{13}C{^{1}H} NMR (125 MHz, $CDCl_3$): δ 184,7, 168.2, 155.7, 146.7, 145.8, 141.6, 139.1, 137.4, 135.0, 133.1, 131.9 (3^1,2^1-CH), 96.5, 96.0 (4 × *meso*-CH), 62.2 (2 × OCH_2), 20.0, 19.7 (7,12,13,18-CH_2), 18.6, 17.4 (7,12,13,18-CH_2CH_3), 14.6 (2 × OCH_2CH_3), 11.4 (8,17-CH_3). ^{1}H NMR (500 MHz, TFA-$CDCl_3$): δ 11.12 (s, 2H, 5,20-H), 10.52 (s, 2H, 10,15-H), 10.11 (s, 2H, 2^1,3^1-H), 4.65 (q, 4H, J = 7.2 Hz, 2 × OCH_2), 4.21 (q, 4H, J = 7.7 Hz, 7,18-CH_2), 4.10 (q, 4H, J = 7.7 Hz, 12,13-CH_2), 3.63 (s, 6H, 8,17-CH_3), 1.73 (t, 6H, J = 7.7 Hz, 12,13-CH_2CH_3), 1.67 (t, 6H, J = 7.7 Hz, 7,18-CH_2CH_3), 1.54 (t, 6H, J = 7.2 Hz, 2 × OCH_2CH_3), −2.60 (br s, 2H, 2 × NH), −2.73 (br s, 1H, NH). ^{13}C{^{1}H} NMR (125 MHz, TFA-$CDCl_3$): δ 168.1, 148.4, 146.7, 146.4, 145.1, 144.5, 142.6, 139.5, 139.0, 137.0, 133.7, 132.6 (2 × tropone-CH), 100.0, 99.5 (4 × *meso*-CH), 65.2 (2 × OCH_2), 20.35 (7,18-CH_2), 20.29 (12,13-CH_2), 17.1 (12,13-CH_2CH_3), 16.1 (7,18-CH_2CH_3), 13.7 (2 × OCH_2CH_3), 11.7 (8,17-CH_3). HRMS (ESI) m/z: $[M + H]^+$ calcd for $C_{41}H_{45}N_4O_5$ 673.3384, found 673.3391. The reaction was repeated five times the scale without any decrease in yield. Tripyrrane **15** (265 mg, 0.362 mmol) was reacted with 3,4-diethyl-2,5-pyrroledicarbaldehyde (65.0 mg, 0.363 mmol) in TFA (5 mL) and dichloromethane (200 mL) and oxidized with DDQ (98%, 85 mg, 0.37 mmol). Following workup and purification as described above, **16** (173.9 mg, 0.259 mmol, 71%) was isolated as a dark green solid.

Tropone-Fused Oxaporphyrin 18. Tripyrrane **15** (53.0 mg, 0.0725 mmol) and 2,5-furandicarbaldehyde (9.0 mg, 0.072 mmol) were reacted under the foregoing conditions. The residue was purified by column chromatography on grade 3 basic alumina, eluting with chloroform and then 1% methanol-chloroform, to give a dark green band. Recrystallization with chloroform-hexanes gave the oxaporphyrin (34.1 mg, 0.0553 mmol, 76%) as a dark green solid, mp > 300 °C. UV−vis (1% Et_3N-CH_2Cl_2; 1.479 × 10^{-5} M): λ_{max}/nm (log ε): 334 (sh, 4.52), 378 (4.86), 445 (4.83), 520 (4.08), 589 (4.03), 617 (3.94), 667 (sh, 4.03), 685 (4.34). UV−vis (2 equiv TFA-CH_2Cl_2): λ_{max}/nm (log ε): 298 (4.32), 338 (sh, 4.41), 362 (sh, 4.56), 406 (sh, 5.13), 418 (5.17), 556 (4.10), 568 (4.10), 606 (4.56). UV−vis (1% TFA-CH_2Cl_2; 9.10 × 10^3 equiv TFA): λ_{max}/nm (log ε): 303 (4.38), 368 (4.71), 406 (sh, 5.04), 423 (5.13), 561 (4.09), 611 (4.58). ^{1}H NMR (500 MHz, TFA-$CDCl_3$): δ 11.12 (s, 2H, 10,15-H), 11.08 (s, 2H, 5,20-H), 10.62 (s, 2H, 2,3-H), 10.23 (s, 2H, 2 × tropone-H), 4.69 (q, 4H, J = 7.2 Hz, 2 × OCH_2), 4.43 (4H, q, J = 7.8 Hz, 8,17-CH_2), 3.90 (s, 6H, 7,18-CH_3), 2.01 (t, 6H, J = 7.8 Hz, 8,17-CH_2CH_3), 1.61 (t, 6H, J = 7.2 Hz, 2 × OCH_2CH_3). ^{1}H NMR (500 MHz, TFA-DMSO-d_6): δ 10.49 (s, 2H, 10,15-H), 10.29 (s, 2H, 5,20-H), 10.12 (s, 2H, 2,3-H), 9.88 (s, 2H, 2 × tropone-H), 4.72 (q, 4H, J = 7.2 Hz, 2 × OCH_2), 4.12 (4H, q, J = 7.7 Hz, 8,17-CH_2), 3.58 (s, 6H, 7,18-CH_3), 1.69 (t, 6H, J = 7.7 Hz, 8,17-CH_2CH_3), 1.63 (t, 6H, J = 7.2 Hz, 2 × OCH_2CH_3), −8.93 (br s, 2H, 2 × NH). ^{13}C{^{1}H} NMR (125 MHz, TFA-$CDCl_3$): δ 185.7, 168.5, 155.1, 151.9, 148.1, 142.4, 140.2, 139.7, 139.5, 136.5, 134.1, 133.0 (2 × tropone-CH), 132.0 (2,3-CH), 104.0 (10,15-CH), 97.6 (5,20-CH), 64.8 (2 × OCH_2), 20.1 (8,17-CH_2), 17.2 (8,17-CH_2CH_3), 14.0 (2 × OCH_2CH_3), 11.8 (7,18-CH_3). ^{13}C{^{1}H} NMR (125 MHz, TFA-DMSO-d_6): δ 182.6, 167.5, 152.9, 149.5, 145,8, 141.7, 140.8, 137.7, 136.7, 132.3 (2,3-CH), 130.5 (2 × tropone-CH), 102.5 (10,15-CH), 96.5 (5,20-CH), 62.4 (2 × OCH_2), 19.2 (8,17-CH_2), 17.4 (8,17-CH_2CH_3), 14.7 (2 × OCH_2CH_3), 11.6 (7,18-CH_3). HRMS (ESI) m/z: $[M + H]^+$ calcd for $C_{37}H_{36}N_3O_6$ 618.2599, found 618.2604.

Tropone-Fused Thiaporphyrin 19. Tripyrrane **15** (53.0 mg, 0.0725 mmol) and 2,5-thiophenedicarbaldehyde (10.2 mg, 0.073 mmol) were reacted under the previously described conditions. Purification by column chromatography on grade 3 basic alumina, eluting with dichloromethane and then 50% dichloromethane-chloroform, afforded a dark orange-brown band. Recrystallization from chloroform-hexanes gave the thiaporphyrin (23.3 mg, 0.0638 mmol, 51%) as an orange-brown solid, mp > 300 °C. UV−vis (CH_2Cl_2; 1.554 × 10^{-5} M): λ_{max}/nm (log ε): 300 (sh, 4.27), 338 (4.37), 386 (4.82), 424 (sh, 4.78), 447 (4.91), 524 (4.21), 628 (3.61), 690 (4.39). UV−vis (100 equiv TFA-CH_2Cl_2): λ_{max}/nm (log ε): 302 (4.38), 429 (5.23), 574 (4.10), 620 (4.38). UV−vis (20% TFA-CH_2Cl_2; 1.73 × 10^5 equiv TFA): λ_{max}/nm (log ε): 310 (sh, 4.34), 381 (4.61), 441 (5.14), 577 (3.92), 630 (4.39), 681 (3.92). ^{1}H NMR (500 MHz, $CDCl_3$): δ 10.38 (s, 2H, 5,20-H), 9.98 (s, 2H, 2,3-H), 9.38 (s, 4H, 2 × tropone-H and 10,15-H), 4.72 (q, 4H, J = 7.2 Hz, 2 × OCH_2), 3.69 (q, 4H, J = 7.7 Hz, 8,17-CH_2), 3.33 (s, 6H, 7,18-CH_3), 1.71 (t, 6H, J = 7.7 Hz, 8,17-CH_2CH_3), 1.67 (t, 6H, J = 7.2 Hz, 2 × OCH_2CH_3), −4.17 (br s, 1H, NH). ^{13}C{^{1}H} NMR (125 MHz, $CDCl_3$): δ 184.7, 167.0, 159.1, 152.5, 149.2, 146.7, 138.3, 135.0, 134.7 (2,3-CH), 132.3, 131.3 (2 × tropone-CH), 129.3, 113.2 (5,20-CH), 98.1 (10,15-CH), 62.4 (2 × OCH_2), 19.6 (8,17-CH_2), 17.3 (8,17-CH_2CH_3), 14.6 (2 × OCH_2CH_3), 11.4 (7,18-CH_3). ^{1}H NMR (500 MHz, TFA-$CDCl_3$): δ 11.53 (s, 2H, 5,20-H), 11.23 (s, 2H, 10,15-H), 10.61 (s, 2H, 2,3-H), 10.35 (s, 2H, 2 × tropone-H), 4.72 (q, 4H, J = 7.2 Hz, 2 × OCH_2), 4.41 (q, 4H, J = 7.7 Hz, 8,17-CH_2), 3.89 (s, 6H, 7,18-CH_3), 2.02 (t, 6H, J = 7.7 Hz, 8,17-CH_2CH_3), 1.62 (t, 6H, J = 7.2 Hz, 2 × OCH_2CH_3). ^{13}C{^{1}H} NMR (125 MHz, TFA-$CDCl_3$): δ 167.8, 153.3, 147.3, 143.2, 142.4, 141.1, 140.8, 138.2, 136.8 (2,3-C), 133.0 (2 × tropone-CH), 111.8 (5,20-CH), 103.7 (10,15-CH), 64.4 (2 × OCH_2), 20.0 (8,17-CH_2), 17.2 (8,17-CH_2CH_3), 14.1 (2 × OCH_2CH_3), 12.0 (7,18-CH_3). HRMS (ESI) m/z: $[M + H]^+$ calcd for $C_{37}H_{36}N_3O_5S$ 634.2370, found 634.2377.

Tropone-Fused Selenaporphyrin 20. Tripyrrane **15** (53.0 mg, 0.0725 mmol) and 2,5-selenophenedicarbaldehyde[29] (13.6 mg, 0.0723 mmol) were reacted as described above. The crude product was purified by column chromatography on grade 3 basic alumina, eluting with dichloromethane, to give a dark orange-brown band. Recrystallization from chloroform-hexanes gave the selenaporphyrin (24.7 mg, 0.0363 mmol, 50%) as a dark orange-brown solid, mp > 300 °C. UV−vis (CH_2Cl_2; 1.628 × 10^{-5} M): λ_{max}/nm (log ε): 344 (sh, 4.43), 387 (4.73), 446 (4.97), 524 (4.29), 628 (3.68), 689 (4.39). UV−vis (1% TFA-CH_2Cl_2; 8.27 × 10^3 equiv TFA): λ_{max}/nm (log ε): 333 (4.39), 453 (5.21), 593 (4.14), 645 (4.28). ^{1}H NMR (500 MHz,

https://doi.org/10.1021/acs.joc.1c02063
J. Org. Chem. 2022, 87, 952−962

$CDCl_3$): δ 10.19 (s, 2H, 5,20-H), 10.04 (s, 2H, 2,3-H), 8.73 (s, 2H, 2 × tropone-H), 8.50 (s, 2H, 10,15-H), 4.76 (q, 4H, J = 7.2 Hz, 2 × OCH_2), 3.37 (q, 4H, J = 7.8 Hz, 8,17-CH_2), 3.18 (s, 6H, 7,18-CH_3), 1.72 (t, 6H, J = 7.2 Hz, 2 × OCH_2CH_3), 1.58 (t, 6H, J = 7.8 Hz, 8,17-CH_2CH_3), −5.45 (br s, 1H, NH). $^{13}C\{^1H\}$ NMR (125 MHz, $CDCl_3$): δ 184.7, 167.0, 160.5, 154.4, 150.6, 146.8, 136.8 (2,3-C), 134.4, 131.1 (2 × tropone-CH), 130.7, 128.5, 116.3 (5,20-C), 98.3 (10,15-C), 62.4 (2 × OCH_2), 19.5 (8,17-CH_2), 17.2 (8,17-CH_2CH_3), 14.7 (2 × OCH_2CH_3), 11.3 (7,18-CH_3). ^1H NMR (500 MHz, TFA-$CDCl_3$): δ 11.53 (s, 2H, 5,20-H), 11.13 (s, 2H, 10,15-H), 10.40 (s, 2H, 2,3-H), 10.29 (s, 2H, 2 × tropone-H), 4.70 (q, 4H, J = 7.1 Hz, 2 × OCH_2), 4.37 (q, 4H, J = 7.7 Hz, 8,17-CH_2), 3.83 (s, 6H, 7,18-CH_3), 2.00 (t, 6H, J = 7.7 Hz, 8,17-CH_2CH_3), 1.61 (t, 6H, J = 7.1 Hz, 2 × OCH_2CH_3). $^{13}C\{^1H\}$ NMR (125 MHz, TFA-$CDCl_3$): δ 185.3, 167.4, 159.5, 152.1, 148.3, 145.3, 142.5, 141.2, 140.4, 139.3 (2,3-C), 136.9, 132.4 (2 × tropone-CH), 116.9 (5,20-C), 103.5 (5,20-C), 64.0 (2 × OCH_2), 20.1 (8,17-CH_2), 17.2 (8,17-CH_2CH_3), 14.2 (2 × OCH_2CH_3), 11.8 (7,18-CH_3). HRMS (ESI) m/z: $[M + H]^+$ calcd for $C_{37}H_{36}N_3O_5Se$ 682.1815, found 682.1824.

Tropone-Fused Benzocarbaporphyrin 21. Tripyrrane **15** (53.0 mg, 0.0725 mmol) and indene dialdehyde **24**[30] (12.5 mg, 0.0727 mmol) were reacted under the foregoing conditions. The crude product was purified by column chromatography on grade 3 basic alumina, eluting initially with dichloromethane and then chloroform, to give a dark green band. Recrystallization with chloroform-hexanes gave the carbaporphyrin (23.4 mg, 0.0354 mmol, 49%) as a dark green solid, mp > 300 °C. UV−vis (1% Et_3N-CH_2Cl_2; 1.001×10^{-5} M): λ_{max}/nm (log ε): 401 (4.47), 432 (sh, 4.47), 460 (4.91), 558 (sh, 3.72), 610 (4.44), 652 (sh, 4.03), 711 (3.41). UV−vis (500 equiv TFA-CH_2Cl_2): λ_{max}/nm (log ε): 315 (4.23), 398 (4.34), 473 (4.67), 509 (4.48), 608 (sh, 3.86), 639 (4.01), 720 (3.73). ^1H NMR (500 MHz, $CDCl_3$): δ 9.05 (s, 2H, 2 × tropone-H), 9.04 (s, 2H, 5,20-H), 8.54−8.52 (m, 2H, 2^1,3^1-H), 8.50 (s, 2H, 10,15-H), 7.80−7.77 (m, 2H, 2^2,3^2-H), 4.76 (q, 4H, J = 7.1 Hz, 2 × OCH_2), 3.57 (q, 4H, J = 7.8 Hz, 8,17-CH_2), 3.20 (s, 6H, 7,18-CH_3), 1.71 (t, 6H, J = 7.1 Hz, 2 × OCH_2CH_3), 1.58 (t, 6H, J = 7.8 Hz, 8,17-CH_2CH_3), −6.99 (br s, 2H, 2 × NH), −9.29 (s, 1H, 21-H). ^1H NMR (500 MHz, $CDCl_3$, 328 K): δ 9.03 (s, 2H, 2 × tropone-H), 8.94 (s, 2H, 5,20-H), 8.50 (s, 2H, 10,15-H), 8.47−8.44 (m, 2H, 2^1,3^1-H), 7.75−7.72 (m, 2H, 2^2,3^2-H), 4.76 (q, 4H, J = 7.1 Hz, 2 × OCH_2), 3.54 (q, 4H, J = 7.7 Hz, 8,17-CH_2), 3.16 (s, 6H, 7,18-CH_3), 1.71 (t, 6H, J = 7.1 Hz, 2 × OCH_2CH_3), 1.60 (t, 6H, J = 7.7 Hz, 8,17-CH_2CH_3), −7.23 (br s, 2H, 2 × NH), −9.64 (s, 1H, 21-H). $^{13}C\{^1H\}$ NMR (125 MHz, $CDCl_3$): δ 184.6, 168.0, 145.6, 141.1, 139.1, 136.8, 136.2, 136.0, 134.6, 133.7, 132.6, 131.5 (2 × tropone-CH), 127.6 (2^2,3^2-CH), 120.9 (2^1,3^1-CH), 108.6 (21-CH), 97.6 (5,20-CH), 93.5 (10,15-CH), 62.3 (2 × OCH_2), 19.2 (8,17-CH_2), 17.0 (8,17-CH_2CH_3), 14.7 (2 × OCH_2CH_3), 11.1 (7,18-CH_3). ^1H NMR (500 MHz, TFA-$CDCl_3$): δ 10.42 (s, 2H, 10,15-H), 10.20 (s, 2H, 5,20-H), 10.09 (s, 2H, 2 × tropone-H), 8.58−8.55 (m, 2H, 2^1,3^1-H), 7.70−7.66 (m, 2H, 2^2,3^2-H), 4.64 (q, 4H, J = 7.1 Hz, 2 × OCH_2), 4.11 (q, 4H, J = 7.7 Hz, 8,17-CH_2), 3.56 (s, 6H, 7,18-CH_3), 1.72 (t, 6H, J = 7.7 Hz, 8,17-CH_2CH_3), 1.57 (t, 6H, J = 7.1 Hz, 2 × OCH_2CH_3), −2.18 (br s, 2H, NH), −6.31 (br s, 1H, 21-H). $^{13}C\{^1H\}$ NMR (125 MHz, TFA-$CDCl_3$): δ 167.2, 145.1, 143.8, 141.8, 141.5, 138.8, 136.5, 136.0, 134.3, 132.5 (2 × tropone-CH), 130.8, 129.3 (2^2,3^2-C), 122.2 (2^1,3^1-C), 121.6, 105.1 (5,20-CH), 93.8 (10,15-CH), 63.5 (2 × OCH_2), 20.0 (8,17-CH_2), 16.7 (8,17-CH_2CH_3), 14.2 (2 × OCH_2CH_3), 11.8 (7,18-CH_3). HRMS (ESI) m/z: $[M + H]^+$ calcd for $C_{42}H_{40}N_3O_5$ 666.2962; found 666.2968.

Tropone-Fused Oxybenziporphyrin 22. Tripyrrane **15** (53.0 mg, 0.0725 mmol) and 5-formylsalicylaldehyde (10.9 mg, 0.0726 mmol) were reacted under the same conditions. Purification by column chromatography on grade 3 basic alumina, eluting with chloroform, gave a dark green band. Recrystallization with chloroform-hexanes afforded the oxybenziporphyrin (30.6 mg, 0.0476 mmol, 65%) as a dark green solid, mp > 300 °C. UV−vis (CH_2Cl_2; 1.948×10^{-5} M): λ_{max}/nm (log ε): 284 (4.42), 306 (4.57), 419 (sh, 4.88), 448 (5.04), 465 (sh, 4.92), 572 (sh, 3.80), 627 (4.74), 676 (4.24), 741 (4.02). UV−vis (1% TFA-CH_2Cl_2; 6.91×10^3 equiv TFA): λ_{max}/nm (log ε): 286 (sh, 4.40), 315 (4.47), 393 (sh, 4.65), 445 (4.93), 573 (sh, 3.77), 629 (4.31), 757 (3.94). UV−vis (10% TFA-CH_2Cl_2; 6.91×10^4 equiv TFA): λ_{max}/nm (log ε): 312 (4.43), 391 (sh, 4.71), 443 (4.94), 582 (sh, 3.87), 634 (4.37), 728 (3.90), 804 (3.97). ^1H NMR (500 MHz, $CDCl_3$): δ 9.81 (s, 1H, 21-H), 9.05 (s, 1H, 14^1-H), 8.98 (1H, s, 13^1-H), 8.74 (s, 1H, 6-H), 8.67 (s, 1H, 16-H), 8.50 (d, 1H, J = 9.3 Hz, 3-H), 8.29 (s, 1H, 11-H), 7.37 (d, 1H, J = 9.3 Hz, 4-H), 4.78−4.72 (m, 4H, 2 × OCH_2), 3.72 (q, 2H, J = 7.8 Hz), 3.58 (q, 2H, J = 7.8 Hz, 9-CH_2), 3.27 (s, 3H, 19-CH_3), 3.24 (s, 3H, 8-CH_3), 1.72−1.66 (m, 9H, 2 × OCH_2CH_3 and 18-CH_2CH_3), 1.52 (t, 3H, J = 7.7 Hz, 9-CH_2CH_3), −6.24 (br s, 1H, NH), −6.59 (1H, br s, NH), −9.12 (1H, s, 22-CH). $^{13}C\{^1H\}$ NMR (125 MHz, $CDCl_3$): δ 187.4, 184.3, 167.5, 167.3, 148.7, 147.5, 147.0 (3-CH), 138.5, 138.4, 137.85, 137.76, 137.6, 137.1, 136.2, 135.89, 135.84, 134.6, 133.2, 131.0 (4-CH), 130.7 (13^1,14^1-CH), 130.5, 126.9, 123.8, 111.8 (22-CH), 111.0 (6-CH), 105.0 (21-CH), 94.2 (16-CH), 91.8 (11-CH), 62.6 (2 × OCH_2), 19.3, 19.2 (9,18-CH_2), 17.0, 16.7 (9,18-CH_2CH_3), 14.64, 14.61 (2 × OCH_2CH_3), 11.7 (19-CH_3), 11.4 (8-CH_3). ^1H NMR (500 MHz, TFA-$CDCl_3$): δ 9.94 (s, 1H, 21-H), 9.46 (s, 1H), 9.45 (s, 1H), 9.26 (s, 1H), 9.25 (s, 1H), 9.16 (s, 1H), 8.71 (dd, 1H, J = 2.0, 9.1 Hz, 4-H), 7.61 (d, 1H, J = 9.1 Hz, 3-H), 4.59 (q, 4H, J = 7.1 Hz, 2 × OCH_2), 3.65−3.59 (m, 4H, 9,18-CH_2), 3.17 (s, 3H), 3.15 (s, 3H) (8,19-CH_3), 1.53−1.45 (m, 12H, 4 × CH_2CH_3), −1.08 (1H, br s, 22-H). $^{13}C\{^1H\}$ NMR (125 MHz, TFA-$CDCl_3$): δ 184.8, 166.63, 166.58, 150.0, 146.9, 145.0, 143.6, 142.6, 142.5, 142.3, 141.4, 138.1, 137.9, 136.7, 136.1, 131.0, 130.9, 126.5, 125.1, 124.4, 122.4, 119.3, 116.0, 96.0, 94.1, 64.44, 64.41, 18.9, 15.5, 15.4, 14.0, 11.51, 11.46. HRMS (ESI) m/z: $[M + H]^+$ calcd for $C_{39}H_{38}N_3O_6$ 644.2755, found 644.2764.

Tropone-Fused Oxypyriporphyrin 23. Tripyrrane **15** (53.0 mg, 0.0725 mmol) and 4-hydroxy-2,6-pyridinedicarbaldehyde[24] (11.0 mg, 0.0728 mmol) were reacted under the previous conditions. Purification by column chromatography on grade 3 basic alumina, eluting with chloroform, gave a dark green band. Recrystallization with chloroform-hexanes gave the oxypyriporphyrin (26.6 mg, 0.0413 mmol, 57%) as a dark green solid, mp > 300 °C. UV−vis (CH_2Cl_2; 8.554×10^{-6} M): λ_{max}/nm (log ε): 279 (4.68), 414 (4.93), 442 (5.14), 616 (sh, 4.50), 651 (4.84), 689 (sh, 3.83). UV−vis (1000 equiv TFA-CH_2Cl_2): λ_{max}/nm (log ε): 275 (4.66), 419 (sh, 4.96), 441 (5.08), 623 (4.50), 658 (4.60), 739 (sh, 3.95). ^1H NMR (500 MHz, $CDCl_3$): δ 10.26 (s, 1H, 21-H), 9.25 (s, 1H, 11 or 16-H), 9.18 (s, 1H), 9.07 (s, 1H) (2× tropone-H), 8.99 (d, 1H, J = 9.3 Hz, 4-H), 8.95 (s, 1H, 6-H), 8.80 (s, 1H, 11 or 16-H), 7.81 (d, 1H, J = 9.3 Hz, 3-H), 4.78−4.72 (m, 4H, 2 × OCH_2), 3.84 (q, 2H, J = 7.7 Hz), 3.73 (q, 2H, J = 7.8 Hz) (9,18-CH_2), 3.40 (s, 3H, 19-CH_3), 3.36 (s, 3H, 8-CH_3), 1.72−1.67 (m, 9H, 2 × OCH_2CH_3 and 9- or 18-CH_2CH_3), 1.59 (t, 3H, CH_2CH_3, 9- or 18-CH_2CH_3), −6.04 (1H, br s, NH), −6.28 (1H, br s, NH). $^{13}C\{^1H\}$ NMR (125 MHz, $CDCl_3$): δ 185.0, 184.4, 167.7, 167.5, 148.1, 147.7, 145.9 (4-CH), 144.9, 140.9, 140.7, 139.9, 137.8, 137.7, 136.8, 136.7, 136.6, 136.2, 136.01, 135.96, 135.5, 135.2, 132.0 (3-CH), 130.76, 130.70 (2 × tropone-CH), 107.7 (6-CH), 102.5 (21-CH), 95.7, 95.0 (11,16-CH), 62.6 (2 × OCH_2), 19.5, 19.4 (9,18-CH_2), 17.2, 17.0 (9,18-CH_2CH_3), 14.63, 14.61 (2 × OCH_2CH_3), 11.6, 11.4 (8,19-CH_3). ^1H NMR (500 MHz, TFA-$CDCl_3$): δ 10.79 (s, 1H, 21-H), 10.32 (s, 1H), 10.29 (s, 1H) (11,16-H), 9.88 (s, 1H), 9.87 (s, 1H) (2 × tropone-H), 9.82 (s, 1H, 6-H), 9.73 (d, 1H, J = 9.3 Hz, 3-H), 8.69 (d, 1H, J = 9.3 Hz, 2-H), 4.68−4.64 (m, 4H, 2 × OCH_2), 4.06−3.98 (m, 4H, 9,18-CH_2), 3.490 (s, 3H), 3.486 (s, 3H) (8,19-CH_3), 1.71−1.65 (m, 6H, 9,18-CH_2CH_3), 1.58−1.55 (m, 6H, 2 × OCH_2CH_3), −0.79 (br s, 1H, NH). $^{13}C\{^1H\}$ NMR (TFA-$CDCl_3$): δ 185.7, 179.6, 167.6, 147.5, 147.4, 146.7, 145.8, 145.2, 145.0, 143.8, 142.4, 142.2, 141.7, 140,6, 137.29, 137.25, 136.8, 135.0, 134.9, 134.8, 134.6, 132.78, 132.75 (2 × tropone-CH), 107.4 (21-CH), 103.2 (6-CH), 101.8, 101.5 (11,16-CH), 65.1 (2 × OCH_2), 19.9 (9,18-CH_2), 16.1 (9,18-CH_2CH_3), 13.8 (2 × OCH_2CH_3), 11.8, 11.7 (8,19-CH_3). HRMS (ESI) m/z: $[M + H]^+$ calcd for $C_{38}H_{37}N_4O_6$ 645.2708, found 645.2715.

https://doi.org/10.1021/acs.joc.1c02063
J. Org. Chem. 2022, 87, 952−962

■ ASSOCIATED CONTENT

Supporting Information

The Supporting Information is available free of charge at https://pubs.acs.org/doi/10.1021/acs.joc.1c02063.

Selected UV−vis, ^{1}H NMR, ^{1}H-^{1}H COSY, HSQC, DEPT-135, ^{13}C{^{1}H} NMR, and mass spectra (PDF)

■ AUTHOR INFORMATION

Corresponding Author

Timothy D. Lash − *Department of Chemistry, Illinois State University, Normal, Illinois 61790-4160, United States;* orcid.org/0000-0002-0050-0385; Email: tdlash@ilstu.edu

Author

Emma K. Cramer − *Department of Chemistry, Illinois State University, Normal, Illinois 61790-4160, United States*

Complete contact information is available at: https://pubs.acs.org/10.1021/acs.joc.1c02063

Notes

The authors declare no competing financial interest.

■ ACKNOWLEDGMENTS

This work was supported by the National Science Foundation under grant CHE-1855240. The NSF is also acknowledged for providing funding for the departmental NMR spectrometers (CHE-0722385) and mass spectrometer (CHE-1337497) under the Major Research Instrumentation (MRI) program.

■ REFERENCES

(1) *The Colours of Life*; Milgrom, L. R., Ed.; Oxford University Press: New York, 1997.

(2) (a) Ding, Y.; Zhu, W.-H.; Xie, Y. Development of Ion Chemosensors Based on Porphyrin Analogues. *Chem. Rev.* **2017**, *117*, 2203−2256. (b) Paolesse, R.; Nardis, S.; Monti, D.; Stefanelli, M.; Di Natale, C. Porphyrinoids for Chemical Sensor Applications. *Chem. Rev.* **2017**, *117*, 2517−2583.

(3) (a) Ono, N.; Ito, S.; Wu, C. H.; Chen, C. H.; Wen, T. C. Nonlinear Light Absorption in *meso*-Substituted Tetrabenzoporphyrin and Tetraarylporphyrin Solutions. *Chem. Phys.* **2000**, *262*, 467−473. (b) Rogers, J. E.; Nguyen, K. A.; Hufnagle, D. C.; McLean, D. G.; Su, W. J.; Gossett, K. M.; Burke, K. M.; Vinogradov, S. A.; Pachter, R.; Fleitz, P. A. Observation and Interpretation of Annulated Porphyrins: Studies on the Photophysical Properties of *meso*-Tetraphenylmetalloporphyrins. *J. Phys. Chem. A* **2003**, *107*, 11331−11339.

(4) (a) Rose, E.; Andrioletti, B.; Zrig, S.; Quelquejeu-Ethève, M. Enantioselective Epoxidation of Olefins with Chiral Metalloporphyrin Catalysts. *Chem. Soc. Rev.* **2005**, *34*, 573−583. (b) Lu, H.; Zhang, X. P. Catalytic C.-H. Functionalization by Metalloporphyrins: Recent Developments and Future Directions. *Chem. Soc. Rev.* **2011**, *40*, 1899−1909. (c) Che, C.-M.; Lo, V. K.-Y.; Zhou, C.-Y.; Huang, J. S. Selective Functionalization of Saturated C-H bonds with Metalloporphyrin Catalysts. *Chem. Soc. Rev.* **2011**, *40*, 1950−1975. (d) Pellissier, H.; Clavier, H. Enantioselective Cobalt-Catalyzed Transformations. *Chem. Rev.* **2014**, *114*, 2775−2823. (e) Gopalaiah, K. Chiral Iron Catalysts for Asymmetric Synthesis. *Chem. Rev.* **2013**, *113*, 3248−3296.

(5) Li, L.-L.; Diau, E. W.-G. Porphyrin-Sensitized Solar Cells. *Chem. Soc. Rev.* **2013**, *42*, 291−304.

(6) (a) Bonnett, R. Photosensitizers of the Porphyrin and Phthalocyanine Series for Photodynamic Therapy. *Chem. Soc. Rev.* **1995**, *24*, 19−33. (b) Ethirajan, M.; Chen, Y.; Joshi, P.; Pandey, R. K. The Role of Porphyrin Chemistry in Tumor Imaging and Photodynamic Therapy. *Chem. Soc. Rev.* **2011**, *40*, 340−362.

(7) (a) Sessler, J. L.; Seidel, D. Synthetic Expanded Porphyrin Therapy. *Angew. Chem., Int. Ed.* **2003**, *42*, 5134−5175. (b) Tanaka, T.; Osuka, A. Chemistry of *meso*-Aryl-Substituted Expanded Porphyrins: Aromaticity and Molecular Twist. *Chem. Rev.* **2017**, *117*, 2584−2640.

(8) (a) Orłowski, R.; Gryko, D.; Gryko, D. T. Synthesis of Corroles and their Heteroanalogs. *Chem. Rev.* **2017**, *117*, 3102−3137. (b) Inokuma, Y.; Osuka, A. Subporphyrins: Emerging Contracted Porphyrins with Aromatic 14π-Electronic Systems and Bowl-Shaped Structures: Rational and Unexpected Synthetic Routes. *Dalton Trans.* **2008**, *37*, 2517−2526. (c) Shimizu, S. Recent Advances in Subporphyrins and Triphyrin Analogues: Contracted Porphyrins Comprising Three Pyrrole Rings. *Chem. Rev.* **2017**, *117*, 2730−2784.

(9) (a) Latos-Grażyński, L. Core-Modified Heteroanalogues of Porphyrins and Metalloporphyrins in *The Porphyrin Handbook*; Kadish, K. M.; Smith, K. M.; Guilard, R., Eds.; Academic Press: San Diego, 2000; *2*, 361−416. (b) Brückner, C.; Akhigbe, J.; Samankumara, L. P. Porphyrin Analogs Containing Non-Pyrrolic Heterocycles in *Handbook of Porphyrin Science - With Applications to Chemistry, Physics, Material Science, Engineering, Biology and Medicine*; ed. Smith, K. M.; Kadish, K. M.; Guilard, R. World Scientific: Singapore, 2014, *35*, 1−275. (c) Chatterjee, T.; Shetti, V. S.; Sharma, R.; Ravikanth, M. Heteroatom-Containing Porphyrin Analogues. *Chem. Rev.* **2017**, *117*, 3254−3328.

(10) Lash, T. D.; Rauen, P. J. Extended Porphyrinoid Chromophores: Heteroporphyrins Fused to Phenanthrene and Acenaphthylene. *Tetrahedron* **2021**, *100*, No. 132481.

(11) Latham, A. N.; Lash, T. D. Synthesis and Characterization of *N*-Methylporphyrins, Heteroporphyrins, Carbaporphyrins, and Related Systems. *J. Org. Chem.* **2020**, *85*, 13050−13068.

(12) Matano, Y.; Imahori, H. Phosphole-Containing Calixpyrroles, Calixphyrins, and Porphyrins: Synthesis and Coordination Chemistry. *Acc. Chem. Res.* **2009**, *42*, 1193−1204.

(13) Lash, T. D. Carbaporphyrinoid Systems. *Chem. Rev.* **2017**, *117*, 2313−2446.

(14) Lash, T. D.; Hayes, M. J.; Spence, J. D.; Muckey, M. A.; Ferrence, G. M.; Szczepura, L. F. Conjugated Macrocycles Related to the Porphyrins. Part 21. Synthesis, Spectroscopy, Electrochemistry and Structural Characterization of Carbaporphyrins. *J. Org. Chem.* **2002**, *67*, 4860−4874.

(15) Lash, T. D. Out of the Blue! Azuliporphyrins and Related Carbaporphyrinoid Systems. *Acc. Chem. Res.* **2016**, *49*, 471−482.

(16) Lash, T. D.; Gilot, G. C.; AbuSalim, D. I. Tropone-fused Carbaporphyrins. *J. Org. Chem.* **2014**, *79*, 9704−9716.

(17) Kreher, R.; Vogt, G.; Schultz, M.-L. Synthesis of 2*H*-Cyclohepta[*c*]pyrrol-6-ones. A Route to 2-Azaazulenes. *Angew. Chem., Int. Ed. Engl.* **1975**, *14*, 821.

(18) Alan Jones, R.; Singh, S. Synthesis and Reduction of 2*H*-Cyclohepta[*c*]pyrrol-6-ones. *Heterocycles* **1976**, *4*, 969−972.

(19) Duflos, J.; Queguiner, G. Reaction de l'acetylene dicarboxylate d'ethyle avec l'oxo-6 (2H) cyclohepta[*c*]pyrrole; mecanismes de formation des adduits. *Tetrahedron* **1985**, *41*, 3303−3311.

(20) Boudif, A.; Momenteau, M. A New Convergent Method for Porphyrin Synthesis Based on a '3 + 1' Condensation. *J. Chem. Soc., Perkin. Trans. 1* **1996**, *1996*, 1235−1242.

(21) Lash, T. D. What's in a Name? The MacDonald Condensation. *J. Porphyrins Phthalocyanines* **2016**, *20*, 855−888.

(22) Medforth, C. J. NMR Spectroscopy of Diamagnetic Porphyrins. *The Porphyrin Handbook*; Kadish, K. M.; Smith, K. M.; Guilard, R., Eds.; Academic Press: San Diego, 2000; *5*, 1−80.

(23) Kodama, T.; Kawashima, Y.; Uchida, K.; Deng, Z.; Tobisu, M. Synthesis and Characterization of 1-Hydroxy-4,5-arene-Fused Tropylium Derivatives. *J. Org. Chem.* **2021**, *86*, 13800−13807.

(24) Lash, T. D.; Chaney, S. T.; Richter, D. T. Conjugated Macrocycles Related to the Porphyrins. Part 12. Oxybenzi- and Oxypyriporphyrins: Aromaticity and Conjugation in Highly Modified Porphyrinoid Structures. *J. Org. Chem.* **1998**, *63*, 9076−9088.

(25) Ghigi, E.; Drusiani, A. Pyrrole aldehyde synthesis. II. *Atti Accad. Sci. Ist Bologna, Classe Sci. Fis.* **1957**, *11*, 14−21.

(26) Barton, D. H. R.; Kervagoret, J.; Zard, S. Z. A Useful Synthesis of Pyrroles from Nitroolefins. *Tetrahedron* **1990**, *46*, 7587−7598.
(27) (a) Tardieux, C.; Bolze, F.; Gros, C. P.; Guilard, R. New One-Step Synthesis of 3,4-Disubstituted Pyrrole-2,5-dicarbaldehydes. *Synthesis* **1998**, 267−268. (b) Li, R.; Lammer, A. D.; Ferrence, G. M.; Lash, T. D. Synthesis, Structural Characterization, Aromatic Properties and Metalation of Neo-Confused Porphyrins, a Newly Discovered Class of Porphyrin Isomers. *J. Org. Chem.* **2014**, *79*, 4078−4093.
(28) Neutralization of the reaction mixture was performed by the dropwise addition of triethylamine. The white fumes resulting from the formation of triethylammonium trifluoroacetate were dispelled with a stream of nitrogen. The reaction mixture was deemed to be neutralized when no additional fumes were formed upon further addition of triethylamine.
(29) Lash, T. D.; Colby, D. A.; Graham, S. R.; Chaney, S. T. Synthesis, Spectroscopy and Reactivity of *meso*-Unsubstituted Azuliporphyrins and their Heteroanalogues. Oxidative Ring Contractions to Carba-, Oxacarba-, Thiacarba- and Selenacarbaporphyrins. *J. Org. Chem.* **2004**, *69*, 8851−8864.
(30) Arnold, Z. Synthetic Reactions of Dimethylformamide. XXII. Formation and Preparation of Formyl Derivatives of Indene. *Collect. Czech. Chem. Commun.* **1965**, *30*, 2783−2792.

https://doi.org/10.1021/acs.joc.1c02063
J. Org. Chem. 2022, 87, 952−962